Ezh2 Inhibitors Reverse Resistance to Gefitinib in Primary Egfr Wild-type Lung Cancer Cells

Hao Gong
Tianjin Medical University General Hospital
Yongwen Li
Tianjin Medical University General Hospital
Yin Yuan
Tianjin Medical University General Hospital
Weiting Li
Tianjin Medical University General Hospital
Hongbing Zhang
Tianjin Medical University General Hospital
Zihe Zhang
Tianjin Medical University General Hospital
Ruifeng Shi
Tianjin Medical University General Hospital
Minghui Liu
Tianjin Medical University General Hospital
Chao Liu
Tianjin Medical University General Hospital
Hongyu Liu
Tianjin Medical University General Hospital
Jun Chen (huntercj2004@qq.com)
Tianjin Medical University General Hospital https://orcid.org/0000-0002-2362-5359

Research

Keywords: non–small-cell lung cancer, enhancer of zeste homolog 2, enhancer of zeste homolog 2 inhibitor, epidermal growth factor receptor-tyrosine kinase inhibitor

Posted Date: June 11th, 2020

DOI: https://doi.org/10.21203/rs.3.rs-33892/v1

Version of Record: A version of this preprint was published at BMC Cancer on December 1st, 2020. See the published version at https://doi.org/10.1186/s12885-020-07667-7.

Abstract

Background: Lung cancer is the leading cause of cancer-related death worldwide. Non–small-cell lung cancer (NSCLC) is the most common type of lung cancer. Traditional anticancer therapies involving epidermal growth factor receptor (EGFR)-tyrosine kinase inhibitors (EGFR-TKIs) have been proven beneficial in the treatment of patients with EGFR mutations. However, patients with EGFR wild-type NSCLC usually fail to respond to EGFR-TKIs. Enhancer of zeste homolog 2 (*EZH2*), a key molecule of the PRC2 complex, plays an important role in epigenetic regulation and is overexpressed in various tumors. *EZH2* inhibitors sensitize various types of tumor cells to antitumor drugs. Therefore, this study aimed to investigate whether the *EZH2* inhibitors GSK343 and DZNep, whencombined with gefitinib, can reverse EGFR-TKI resistance in EGFR wild-type NSCLC.

Methods:*EZH2* expression was evaluated using the RNA sequencing dataset of NSCLC patients (502 lung squamous cell carcinoma cases including 49 paracancerous lung tissues and 513 lung adenocarcinoma cases including 59 paracancerous lung tissues) from The Cancer Genome Atlas (TCGA). We simultaneously also verified *EZH2* expressionin 40 NSCLC samples and their corresponding paracancerous lung tissues from our institution via quantitative PCR. The lung adenocarcinoma cell lines A549 and H1299 were treated with *EZH2*-specific small interfering RNA or *EZH2* inhibitors and subjected to analyses of cell viability and apoptosis as well as of EGFR pathway protein expressions by western blotting.

Results: *EZH2* was upregulated in human NSCLC tissues and was correlated with poor prognosis in patients with lung adenocarcinoma based on data from both TCGA and our institution. Both *EZH2* inhibitors sensitized A549 and H1299 cells to gefitinib and suppressed cell viability and proliferation *in vitro*by downregulating the phosphorylation of EGFR and AKT and inducing cell apoptosis. Co-administration of *EZH2* inhibitors (GSK343 or DZNep) with gefitinib exerted stronger inhibitory effects on tumor activity, cell proliferation, and cell migration than single drug administration *in vitro* and *in vivo*.

Conclusion: Co-administration of *EZH2* inhibitors with EGFR-TKIs may be feasible for the treatment of EGFR wild-type NSCLC in patients who refuse traditional chemotherapy.

Background

Lung cancer is the leading cause of cancer-related death worldwide and is characterized by early metastasis, high mortality, and poor survival [1]. Non–small-cell lung cancer (NSCLC) including lung adenocarcinoma (LUAD), squamous cell carcinoma (LUSC), and large-cell carcinoma accounts for approximately 85% of all lung cancer cases [2]. Despite advances in the clinical diagnosis of lung cancer and the associated therapeutic strategies, patients with late-stage disease have a 5-year overall survival (OS) rate of only 11%–16% [2, 3]. The lack of biomarkers to facilitate the diagnosis of early-stage disease and cancer metastasis remains one of the crucial challenges in NSCLC therapy [4]. Therefore, a profound understanding of the molecular mechanisms contributing to the development and progression of NSCLC is essential for developing specific diagnostic methods and designing individualized and effective physiological strategies.

Targeted drugs such as epidermal growth factor receptor (EGFR)-tyrosine kinase inhibitors (EGFR-TKIs) represent one of the vital advances in lung cancer treatment. EGFR is an essential receptor tyrosine kinase that can regulate cell proliferation and differentiation, and its abnormal activation contributes to a variety of human cancers [18]. EGFR signaling can be activated constitutively by a gene mutation, gene amplification, or both, and this event has been shown to be closely related to the occurrence, progression, and poor prognosis of NSCLC [19, 20]. EGFR-driven mutation rate is 15% in the Caucasian population and 40%–62% in the Asian population [21]. The discovery of EGFR-activating mutations in NSCLC and the successful use of EGFR-TKIs have shifted the focus of cancer treatment from empirical cytotoxic chemotherapy to molecularly targeted therapies. The current common practices involve the administration of EGFR-TKIs as first-line treatment to patients with EGFR-sensitive mutations because these drugs have been shown to considerably prolong progression-free survival while causing fewer adverse effects than chemotherapy [22]. EGFR-TKIs have also been approved as the second- or third-line treatment for EGFR wild-type (EGFR-wt) NSCLC. However, the use of these targeted drugs beyond the first line of treatment remains controversial, particularly for the treatment of EGFR-wt NSCLC.

Recently, histone post-translational modifications such as acetylation, methylation, and phosphorylation were found to play important roles in tumorigenesis [8]. Histones are considered important centers of epigenetic regulation. Polycomb group proteins such as PCR2 act as transcriptional repressors by silencing specific sets of genes via chromatin modification and thereby play key roles in various epigenetic phenomena. Enhancer of zeste homolog 2 (*EZH2*), a key component of polycomb suppression complex 2 (PRC2), is responsible for monomethylation, dimethylation, and trimethylation of histone H3K27 [9]. *EZH2* overexpression has been described in a variety of human cancers including NSCLC [10-12]. *EZH2* can also promote the development and progression of cancer via chromatin modification including the epigenetic activation of the oncogenic signaling cascade and silencing of tumor suppressor genes; it has been implicated in cell proliferation, differentiation, invasion, and metastasis [11, 13, 14]. *EZH2* overexpression is associated with poor prognosis in lung cancer; thus, it is considered an attractive therapeutic target [15, 16]. In addition, various *EZH2* inhibitors have been developed and the safety and antitumor efficacies of these drugs are being investigated in ongoing research and clinical studies. Commonly used *EZH2* inhibitors can be classified into two types. The first type comprises S-adenosyl-L-homocysteine (SAH) hydrolase inhibitors, which block the hydrolysis of SAH into homocysteine and adenosine and indirectly inhibit the methionine cycle and S-adenosyl-L-methionine (SAM) regeneration, leading to the consumption of *EZH2* via the bypass route. 3-DeazaneplanocinA (DZNep) is the most representative of this drug type [17]. The second type of *EZH2* inhibitor comprises competitive SAM inhibitors. These drugs compete with SAM for binding sites on H3K27, decreasing the number of bound SAMs. In turn, the activities of SAM-dependent methyltransferases are inhibited and the trimethylation of H3K27 is blocked. GSK343 and GSK126 are the most well-known representatives of this drug type.

EZH2 is overexpressed in various tumors including lung cancer. *EZH2* inhibitors have been reported to sensitize many types of tumor cells to antitumor drugs. In the present study, we investigated the role of *EZH2* inhibitors in reversing acquired resistance to gefitinib in EGFR-wt lung cancer cells. Briefly, we demonstrated that *EZH2* was upregulated in human NSCLC tissues and that this upregulation was correlated with poor prognosis in patients with LUAD. GSK343 and DZNep both sensitized EGFR-wt LUAD cells (A549 and H1299) to gefitinib and suppressed cell viability and proliferation *in vitro* by downregulating the phosphorylation of EGFR and AKT and inducing cell apoptosis. The co-administration of these *EZH2* inhibitors with gefitinib exerted stronger inhibitory effects on tumor activity than the administration of either drug alone.

Materials And Methods

Patients and tissue specimens

A total of 40 paired NSCLC and their paracancerous lung tissues were obtained from patients who were diagnosed with NSCLC based on histopathological evaluations and had undergone surgery at Tianjin Medical University General Hospital (TJMUGH) between January 2010 and December 2011. Among these, 16 patients were diagnosed with primary LUAC and 24 with primary LUSC. In each patient, lung cancer staging was performed according to the AJCC Cancer Staging Manual, 8th edition, and findings of physical examination; surgical resection; and computed tomography of the chest, abdomen, pelvis, and brain. All collected tissue samples were immediately snap-frozen in liquid nitrogen and stored at −80°C prior to RNA extraction. Basic demographic and clinical information such as sex, age, smoking history, TNM stage, lymph node metastasis, and prognostic data were also collected from medical records.

Download ofThe Cancer Genome Atlas (TCGA) data and preprocessing of RNA-seq data

All next-generation RNA sequencing (RNA-seq) data corresponding to NSCLC cases in the TCGA database were analyzed using TCGA-Assembler. Data of a total of 513 patients with LUAD (including 59 paracancerous lung tissues) and 502 patients with LUSC (including 49 paracancerous lung tissues) were analyzed. Transcripts per million (TPM) was calculated and normalized using the Tag count comparison package (version 1.6.5; http://www.bioconductor.org/packages/release/bioc/html/TCC.html) [23]. The following clinicopathological data evaluated during the follow-up of each patient were obtained from the TCGA NSCLC clinical database: survival status, survival time, age, sex, histology, smoking status, lymph node metastasis, clinical stage, and tumor recurrence. TNM staging was performed according to the AJCC Cancer Staging Manual, 8th edition. Next, the patients were divided into high *EZH2* (greater than or equal to the median) and low *EZH2* (less than the median) expression groups. Kaplan–Meier survival curves and the log-rank test were performed to analyze univariate survival distribution.

Cells culture and treatment

The human LUAD cell line A549 was purchased from the American Type Culture Collection (Manassas, VA, USA). Other human LUAD cell lines (H1299, H1975, HCC827, H1650, and H2030) and the normal human bronchial epithelial cell line BEAS-2B were obtained from the Institute of Biochemistry and Cell Biology of the Chinese Academy of Sciences (Shanghai, China). The H460 and A549 cell lines harbor a *KRAS* mutation; HCC827 and H1650 harbor an *EGFR* exon 19 deletion; *H1299* harbors a p53 deletion or rearrangement mutation; H1975 harbors *EGFR* exon 21 mutation (L858R) and exon 20 (T790m) mutations; H1792 harbors a *TP53* splice mutation and *EGFR* exon 21 (L858R) and exon 20 (T790m) mutations; and H2030 harbors *EGFR* exon 21 (L858R) and *KRAS* mutations. All cell lines were maintained in RPMI 1640 medium supplemented with 10% fetal bovine serum (FBS), 100 IU/ml penicillin, and 100 μg/ml streptomycin (Invitrogen, Carlsbad, CA, USA). All cells were cultured at 37°C in humidified atmosphere containing 5% CO_2. Cells were transfected with small interfering RNAs (siRNAs) specific for *EZH2*; 21-bp (including a 2-deoxynucleotide overhang) siRNA duplexes were purchased from RiboBio (Guangzhou, China). An unrelated siRNA containing a 19-bp scrambled sequence was used as a negative control siRNA. Transfection was performed using 10 nM siRNA oligonucleotide duplexes and Lipofectamine 2000 (Invitrogen) according to the manufacturer's recommendations. Gefitinib (ZD1839), GSK343, and DZNep HCl were obtained from Selleck Chemicals LCC (Houston, TX, USA). Cells were seeded in different culture plates. When the cell confluence level exceeded 60%, *EZH2*-specific siRNA or scrambled control siRNA was transfected using Lipofectamine MAX (Invitrogen) according to the manufacturer's instructions.

Cell Counting Kit-8 (CCK-8) assay

CCK-8 assay (Beyotime) was performed according to the manufacturer's instructions as a quantitative measure of cell proliferation and determinant of the half-maximal inhibitory concentration (IC_{50}) of each drug in each cell line. Briefly, 5000 cells were seeded in each well of a 96-well flat-bottomed plate and incubated for 24 h. Next, different concentrations of gefitinib, GSK343, DZNep, GSK+gefitinib (G+g), and DZNep+gefitinib (D+g) were added to different wells. After 48 h of incubation at 37°C, 10 μl CCK-8 (5 mg/ml) was added to each well and the cells were incubated for another 1 h. Absorbance was measured at 450 nm using a microplate reader (SpectraMax M5, Molecular Devices, Sunnyvale, CA, USA). The experiments were repeated at least three times.

5-Ethynyl-2'-deoxyuridine (EdU) staining

EdU staining involves the incorporation of the nucleoside analog uridine into a newly synthesized DNA strand and detection of the S phase of the cell cycle. This assay can also indirectly reflect cell proliferation. The Cell-Light™ EdU stain kit was obtained from RiboBio, and staining was performed according the manufacturer's instructions. Briefly, the cells were incubated with 50 μM EdU for 2 h, washed twice with phosphate-buffered saline (PBS), and fixed with 4% paraformaldehyde. Next, the proliferated cells were infiltrated with 0.5% Triton X-100, washed twice with PBS, and stained. Subsequently, the cells were analyzed using a fluorescence microscope equipped with a single interference filter set. The red (Apollo)-stained, EdU-labeled cells represent cells is in a state of active division. Blue color represent nuclear staining with Hoechst 33342.

Colony formation assay

Regarding colony formation assay, 500 cells were seeded into each well of a 6-well plate and incubated at 37°C for 24 h. Next, the cells were treated with gefitinib, GSK343, DZNep, G+g, or D+g in medium and incubated at 37°C for 48 h. The concentration of each drug was set as half the IC_{50} value, and normal medium was used as a negative control (NC). After 48 h of drug treatment, the plates were washed twice with PBS, filled with fresh drug-free medium, and incubated for another 21 days. Finally, the plates were washed twice with PBS and stained with 0.5% crystal violet at room temperature for 30 min. The number of colonies (defined as >50 cells) was calculated in each group.

Flow cytometry analysis of apoptosis and cell cycle

Cells (2×10^5 cells/well) were seeded into 6-well plates and cultured for 24 h. Different treatments (NC, GSK343, DZNep, gefitinib, G+g, and D+g) were added at various concentrations, after which the cells were cultured for another 48 h. Regarding apoptosis assay, cells were stained using the Annexin V-FITC Apoptosis Analysis Kit (BD Biosciences, San Jose, CA, USA) and analyzed using the FACSAria™ flow cytometer (BD Biosciences). Regarding cell cycle assay, cells were trypsinized and fixed in 70% ice-cold ethanol overnight. Subsequently, cells were treated with DNase-free ribonuclease (TaKaRa, Beijing, China), stained with propidium iodide (PI; BD Biosciences), and analyzed using the FACSAria™ flow cytometer (BD Biosciences) equipped with ModFit LT (Topsham, ME, USA).

Wound healing assay

H1299 cells were seeded in six-well plates. Once the cells reached 90%–100% confluency, a 200-μL sterile pipette tip was scraped across the confluent cell layer to create an artificial wound. The suspended cells were removed by washing with sterile PBS. Subsequently, medium containing different drugs (NC, GSK343, DZNep, gefitinib, G+g, and D+g) was added to the wells, and the plates were cultured for another 48 h. The initial gap length after scratching (0 h) and residual gap length (24–48 h) were observed under an inverted microscope. Wound closure was calculated using the following formula: (0-h wound width − 24-h wound width) / 0-h wound width. The results of three independent experiments were averaged.

Transwell invasion assay

Regarding cell invasion assay, the upper surfaces of the polycarbonic membranes of Transwell® filters (Corning, NY, USA) were coated with 100 μl of 300 μg/mL Matrigel. Next, 1×10^5 cells were seeded in each upper chamber along with serum-free medium mixed with different drug treatments, and 600 μL medium containing 10% FBS were added to each lower chamber. The cells were incubated at 37°C in a humidified incubator with 5% CO_2 for 24 h. Cells that migrated to the under membranes of the filters were fixed in methanol and stained with 0.1% crystal violet. The Nikon TE2000 microscope (Tokyo, Japan) at 100× magnification was used to collect five randomly selected visual field images. The experiments were performed in triplicate.

Tumor xenografts and OS analysis

Female BALB/c athymic nude mice (4–5 weeks old) were purchased from the Experimental Laboratory Animal Center of Beijing University (Beijing, China). All mice were maintained under specific pathogen-free conditions and were examined prior to starting the study to ensure that they were healthy and could be adapted for tumor implantation. A total of 2×10^6 A549 cells were subcutaneously injected into the left flank of each mouse to establish a tumor xenograft model. When the tumors reached a volume of 200 mm^3, the mice were randomly distributed into the following six groups (10 mice/group). A vehicle group was administered 0.5% methylcellulose 400 (Wako Pure Chemical Industries, Ltd., Osaka, Japan) and sodium lactate buffer via daily oral gavage. A GSK343 group was administered 4 mg/kg GSK343 in 100 μL of corn oil (Santa Cruz Biotechnology, Dallas, TX, USA) via intraperitoneal injection every alternate day. a DZNep group was administered 2 mg DZNep/kg in 100 μL of corn oil via intraperitoneal injection every alternate day. A gefitinib group was administered 100 mg/kg gefitinib/day dissolved in 0.5% methylcellulose 400 and sodium lactate buffer via daily oral gavage. A G+g group was administered 4 mg/kg GSK343 in 100 μL corn oil via intraperitoneal injection every alternate day and 100 mg/kg gefitinib/day in 0.5% methylcellulose 400 and sodium lactate buffer via daily oral gavage. A D+g group was administered 2 mg/kg DZNep in 100 μL corn oil via intraperitoneal injection every alternate day and 100 mg/kg gefitinib/day in 0.5% methylcellulose 400 and sodium lactate buffer via daily oral gavage. All four groups received treatment for 28 days. Tumor size was measured every alternate day. Tumor volume (V) was calculated by measuring tumor length (L) and width (W) with a caliper and using the following formula: $V = (L \times W2) \times 0.5$ [24].

Immunohistochemistry

Xenograft tumor tissues were fixed overnight in 4% formalin, dehydrated with ethanol, and embedded in paraffin. Next, 4-μm-thick tissue slices were first dewaxed with xylose and rehydrated using an alcohol solution gradient. After a 10-min blocking step with normal goat serum, the tissue slices were incubated with a primary antibody specific for *EZH2* (Cell Signaling Technology, Beverly, MA, USA) for 1 h at room temperature, washed with PBS, and incubated with a horseradish peroxidase (HRP)-conjugated secondary antibody (ZSJQ Corp, Beijing, China) for 60 min. Finally, the sections were incubated with 3,3'-diaminobenzidine for 3 min at room temperature and counterstained with hematoxylin.

RNA extraction and quantitative PCR (qPCR) assays

Total RNA was extracted from patient tissue samples or cultured cells using the TRIzol reagent (Invitrogen) according to the manufacturer's instructions. RNA was quantified using a spectrophotometer (Beckman, USA), and RNA quality was assessed using denaturing 1.2% agarose gel electrophoresis. Subsequently, 2 μg of extracted RNA was reverse transcribed in a final reaction volume of 20 μl using random primers under standard conditions specified for the PrimeScript RT reagent Kit (TaKaRa) and reverse transcriptase (Promega, Beijing, China). We used the Power SYBR Green PCR Master Mix (Applied Biosystems, Foster City, CA, USA) to determine *EZH2* and *EGFR* expression levels according to the manufacturer's instructions. Results were normalized to the expression of glyceraldehyde-3-phosphate dehydrogenase (*GAPDH*). qPCR assays and data collection were performed using the ABI 7500 real-time PCR system (Applied Biosystems). All gene primers were obtained from SBS Genetech (Beijing, China). Performance analysis was conducted using the $2^{-\Delta\Delta CT}$ method.

Protein isolation and western blotting

Cells were washed twice with ice-cold PBS and lysed in RIPA buffer [(1× PBS, 1% NP40, 0.5% sodium deoxycholate, 0.1% sodium dodecyl sulfate (SDS)) supplemented with 2 mM PMSF (Thermo Fisher Scientific, Inc., Waltham, MA, USA). We used a BCA protein assay kit (Pierce Biotechnology, Rockford, IL, USA) to measure protein concentrations. Next, 30 μg of each protein extract was denatured and separated using 10% SDS-polyacrylamide gel electrophoresis and electrophoretically transferred onto polyvinylidene fluoride membranes (Millipore, Lake Placid, NY, USA). The membranes were blocked in 5% non-fat milk and incubated overnight at 4°C in dilutions of the following primary antibodies: rabbit anti-human *EZH2* (dilution, 1:1000; Cell Signaling Technology), mouse anti-human β-actin (1:3000; Sigma-Aldrich, St. Louis, MO, USA), rabbit anti-human EGFR (1:1000; Cell Signaling Technology), rabbit anti-human phospho (p)-EGFR (1:1000; Cell Signaling Technology), rabbit anti-human AKT (1:1000; Cell Signaling Technology), rabbit anti-human p-AKT (1:1000; Cell Signaling Technology), rabbit anti-human P38-MAPK (1:1000; Cell Signaling Technology), rabbit anti-human p-P38-MAPK (1:1000; Cell Signaling Technology), rabbit anti-human BCL-2 (1:1000; Cell Signaling Technology), rabbit anti-human Bax (1:1000; Cell Signaling Technology), rabbit anti-human caspase-3 (1:1000; Cell Signaling Technology), rabbit anti-human P62 (1:1000; Cell Signaling Technology),rabbit anti-human mTOR (1:1000; Cell Signaling Technology), and rabbit anti-human p-mTOR (1:1000; Cell Signaling Technology). Subsequently, the membranes were exposed to an HRP-conjugated secondary antibody (1:1000 dilution; Thermo Fisher Scientific, Inc.) at room temperature for 1 h. Finally, the Pierce ECL Substrate (Thermo Fisher Scientific, Inc.) was used to visualize the bands.

Statistical analysis

Statistical analysis was performed using the SPSS software package, version 21.0 (IBM Corp., Armonk, NY, USA). Data are presented as mean ± standard deviation of independent experiments. Kaplan–Meier survival analysis was performed to estimate OS. Univariate cox regression analysis and subsequent multivariate analysis using the likelihood ratio were performed to identify significant variables. The statistical significance of differences between two groups was analyzed using Student's *t*-test. All *P*-values obtained in this study were two tailed, and the statistical significance level was set at *P*-value of <0.05.

Results

EZH2 is strongly expressed in primary lung cancer tissues

EZH2 overexpression has been reported in multiple tumor types. To determine of *EZH2* expression level in NSCLC tumor tissues compared with that in paracancerous lung tissues, LUAD tissues from 513 patients (including 59 paired tumor and paracancerous lung tissues) and LUSC tissues from 502 patients (including 49 paired tumor and paracancerous lung tissues) were collected from the TCGA database. The original analysis of RNA expression indicated considerably higher *EZH2* expression levels in lung cancer tissues than in the paracancerous lung tissues ($P< 0.01$, Figure 1A). As shown in Figure 1B, the TPM of *EZH2* (15.55 ± 13.28) was much higher in LUAD tissues than in the paracancerous lung tissues (2.53 ± 1.11; $P< 0.001$); similarly, the TPM of *EZH2* (28.57 ± 19.49) was much higher in LUSC tissues than in the paracancerous lung tissues (2.94 ± 1.75; $P< 0.01$). To verify the results of TCGA data analysis, we extracted RNA from NSCLC and their paracancerous lung tissues collected from TJMUGH cohort and verified *EZH2* expression using qPCR. Notably, the *EZH2* expression level in NSCLC tissues (n = 40; $2^{-\Delta\Delta CT}$ = 0.09 ± 0.1) was much higher than that in paracancerous lung tissues ($2^{-\Delta\Delta CT}$ = 0.01 ± 0.01; $P < 0.01$, Figure 1C). Western blotting revealed higher *EZH2* expression levels in NSCLC cell lines, particularly A549, HCC827, and H1299, than in the normal bronchus epithelial cell line BEAS-2B (Figure 1D).

Correlation between *EZH2* expression level and clinicopathological characteristics in NSCLC

To investigate the correlation between the *EZH2* expression level and clinicopathological characteristics of NSCLC, we analyzed the data of 352 patients with LUAD and 409 with LUSC from the TCGA cohort and 40 patients with NSCLC from the TJMUGH cohort. A correlation was found between *EZH2* expression level and T stage in patients with LUAD. Higher *EZH2* expression levels were observed in smaller tumors (T1–T2) than in larger tumors (P = 0.033, Table 1). *EZH2* expression was correlated with a history of smoking (P = 0.012) in patients with LUAD. However, no other correlations were observed between *EZH2* expression level and other clinicopathological characteristics of patients with LUAD such as age, sex, lymphatic metastasis status, distant metastasis, TNM stage, and tumor recurrence status . Moreover, we observed no significant associations between *EZH2* expression and the clinicopathological characteristics of patients with LUSC. We obtained similar results in an analysis of 40 patients with NSCLC from the TJMUGH cohort, irrespective of the NSCLC subtype (Table1).

Table 1
Clinicopathological characteristics of NSCLC patients based on the EZH2 expression in TCGA and TJMUGH cohort

	LUAD in TCGA cohort (n=352)			LUAD in TJMUGH cohort (n=16)			LUSC in TCGA cohort (n=409)			LUSC in TJMUGH cohort (n=24)		
Characteristics	Low EHZ2 level (n=176)	HighEHZ2 level (n=176)	X2 test (P-value)	Low EHZ2 level (n=8)	High EHZ2 level (n=8)	X2 test (P-value)	Low EZH2 level(n=205)	High EHZ2 level (n=204)	X2 test (P-value)	Low EZH2 level(n=12)	High EHZ2 level (n=12)	X2 test (P-value)
Age (%)												
≤65	73 (41.5)	93 (52.8)	0.098	4 (50)	2 (25)	0.608	84 (41.0)	77 (37.7)	0.225	5 (41.7)	10 (83.3)	0.089
>65	97 (55.1)	79 (44.9)		4 (50)	6 (75)		120 (58.5)	122 (59.8)		7 (58.3)	2 (16.7)	
Unknown	6 (3.4)	4 (2.3)					1 (0.5)	5 (2.5)				
Gender(%)												
Male	85 (48.3)	90 (51.1)	0.670	6 (75)	4 (50)	0.608	156 (76.1)	149 (73.0)	0.497	10 (83.3)	11 (73.0)	1.000
Female	91 (51.7)	86 (48.9)		2 (25)	4 (50)		49 (23.9)	55 (27)		2 (16.7)	1 (27)	
T stage (%)												
T1-T2	143 (81.3)	125 (71.0)	0.033*	6 (75)	6 (75)	1.000	172 (83.9)	162 (79.4)	0.253	11 (91.7)	8 (66.7)	0.317
T3-T4	33 (16.5)	51 (29.0)		2 (25)	2 (25)		33 (16.1)	42 (20.6)		1 (8.33)	4 (33.3)	
Lymph node metastasis (%)												
Without	116 (65.9)	106 (60.2)	0.320	4 (50)	4 (50)	1.000	131 (63.9)	129 (63.2)	0.918	7 (58.3)	8 (66.7)	0.414
With	60 (18.8)	70 (39.8)		4 (50)	4 (50)		74 (36.1)	75 (36.8)		5 (41.7)	4 (33.3)	
Distant metastasis (%)												
No distant metastasis	168 (95.5)	162 (92)	0.186	8 (100)	8 (100)		200 (97.6)	203 (99.5)	0.215	12 (100)	12 (100)	
Distant organs metastasis	8 (4.5)	14 (8.0)					5 (2.4)	1 (0.5)				
TNM stage(%)												
I+II	105 (96.3)	108 (99.1)	0.116	5 (62.5)	5 (62.5)	1.000	165 (80.5)	167 (81.9)	0.409	8 (66.7)	7 (58.3)	0.414
III+IV	4 (3.7)	1 (0.9)		3 (37.5)	3 (37.5)		40 (19.5)	37 (18.1)		4 (33.3)	5 (41.7)	
Tumor recurrence (%)												
With tumor	34 (19.3)	37 (21.0)	0.733	2 (75)	1 (12.5)	1.000	45 (22.0)	32 (15.7)	0.240	4 (33.3)	2 (16.7)	0.640
Tumor free	99 (56.3)	102(58.0)		6 (25)	7 (87.5)		99 (8.3)	102 (50)		8 (66.7)	10 (83.3)	
Unknown	43 (24.4)	37 (21.0)					61 (29.8)	70 (34.3)				
Smoker history (%)												
Never smokers	26 (14.8)	24 (13.6)	0.012*	5 (62.5)	5 (62.5)	0.619	7 (3.4)	8 (3.9)	0.963	5 (41.6)	2 (16.7)	0.371
Smokers	139 (79)	151 (85.8)		3 (37.5)	3 (37.5)		192 (93.7)	190 (93.1)		7 (58.3)	10 (83.3)	
Unknown	11(6.3)	1(0.6)					6 (2.9)	6 (2.9)				

LUAD:lung adenocarcinoma;LUSC:Lung squamous cell carcinoma;TCGA: The Cancer Genome Atlas

High *EZH2* expression level is associated with poor prognosis in LUAD

Next, OS was estimated using Kaplan–Meier survival analysis and compared using the log-rank test to analyze the associations of *EZH2* expression level with OS outcomes. Analysis of TCGA data revealed that among patients with LUAD, the high *EZH2* expression group had a much lower OS than the low *EZH2* expression group (log-rank test, $P = 0.041$; Figure 1E). Univariate analysis identified *EZH2* expression, age, T stage, lymph node metastasis, distant metastasis, TNM classification, and tumor recurrence as independent prognostic factors for OS in patients with LUAD (log-rank test,$P = 0.041$, 0.026, <0.01, <0.01, 0.038, <0.01, and <0.01, respectively; Table2). No significant correlations were observed between OS and other factors such as sex and smoking status. In patients with LUSC, tumor recurrence status, TNM classification, and smoking status were identified as independent prognostic factors for OS (log-rank test ,$P = 0.020$, 0.01 and 0.048, respectively). Multivariate analysis identified *EZH2* expression, age, T stage, lymph node metastasis, and tumor recurrence to be significantly correlated with prognosis in patients with LUAD (log-rank test,$P = 0.048$, 0.031, 0.026, <0.01, and <0.01, respectively), whereas only tumor recurrence was identified to be significantly correlated with prognosis in patients with LUSC (log-rank test,$P < 0.01$). Taken together, these results indicated that *EZH2* expression level is correlated with prognosis. As shown in Table3, the mean and median OS in the low *EZH2* expression group was 96.95 and 50.93 months, respectively. The mean and median OS in the high *EZH2* expression group was 65.88 and 43.93 months, respectively. However, in patients with LUSC, *EZH2* expression was not significantly correlated with prognosis (Figure 1F, log-rank test, $P = 0.821$). The mean and median OS was 75.31 and 61.37 months in the low *EZH2* expression group and 74.62 and 65.83 months in the high *EZH2* expression group, respectively (Table3).

Table 2
Univariate and multivariate Cox hazard regression in TCGA cohort

Pathological type	Characteristics	Univariate analysis Hazard Ratio (95%CI)	P value	Multivariate analysis Hazard Ratio (95%CI)	P value
LUAD	EZH2 expression	1.412 (1.013-1.967)	0.041*	1.386 (0.976-1.968)	0.048*
	Age	1.013 (1.001-1.024)	0.026*	1.029 (0.748-1.417)	0.031*
	Gender	0.951 (0.684-1.323)	0.767	1.043 (0.744-1.463)	0.807
	T stage	2.619 (1.743-3.936)	0.000*	1.753 (1.069-2.872)	0.026*
	Lymph node metastasis	2.661 (1.906-3.713)	0.000*	2.330 (1.567-3.464)	0.000*
	Presence of distant metastasis	1.936 (1.092-3.434)	0.038*	1.215 (0.630-2.343)	0.560
	TNM classification	2.775 (1.968-3.913)	0.000*	1.365 (0.838-2.225)	0.212
	Tumor recurrence	1.315 (1.167-1.482)	0.000*	1.282 (1.131-1.454)	0.000*
	Smoker status	1.083 (0.826-1.419)	0.569	0.930 (0.689-1.255)	0.635
LUSC	EZH2 expression	0.966 (0.717-1.302)	0.821	0.956 (0.703-1.299)	0.773
	Age	1.196 (0.898-1.594)	0.219	1.306 (0.966-1.765)	0.083
	Gender	0.718 (0.497-1.037)	0.069	0.765 (0.528-1.109)	0.157
	T stage	1.451 (1.004-2.096)	0.056	1.111 (0.716-1.724)	0.639
	Lymph node metastasis	1.098 (0.808-1.491)	0.552	0.900 (0.623-1.301)	0.576
	Presence of distant metastasis	2.506 (0.925-6.791)	0.114	1.839 (0.632-5.351)	0.264
	TNM classification	1.546 (1.085-2.203)	0.020*	1.326 (0.800-2.197)	0.274
	Tumor recurrence	1.369 (1.229-1.524)	0.000*	1.343 (1.202-1.500)	0.000*
	Smoker status	0.619 (0.366-1.048)	0.048*	0.765 (0.528-1.109)	0.127

Table 3
EZH2 expression levels associated with NSCLC overall survival in TCGA cohort and TJMUGH cohort

	Pathological type	Factors	n	Mean survival (Months)	Median survival (Months)	Univariate analysis P value
TCGA chort	LUAD	Low EZH2 expression	176	96.95	50.93	0.041*
		High EZH2 expression	176	65.88	43.93	
	LUSC	Low EZH2 expression	205	75.31	61.37	0.821
		High EZH2 expression	204	74.62	65.83	
TJMUGH chort	LUAD	Low EZH2 expression	8	65.77	63.25	0.393
		High EZH2 expression	8	48.22	32.54	
	LUSC	Low EZH2 expression	12	54.03	45.21	0.152
		High EZH2 expression	12	40.48	35.57	

Clinical data analysis did not identify a significant difference in OS between the high and low *EZH2* expression groups for LUAD or LUSC (log-rank test, P = 0.393 and 0.152, respectively; Figure 1G and H). However, patients with either type of cancer in the high *EZH2* expression group tended to have shorter median and mean OS than those in the low *EZH2* expression group (48.22 and 32.54 months vs. 65.77 and 63.25 months in LUAD, respectively; 40.48 and 35.57 months vs 54.03 and 45.1 months in LUSC, respectively; Figure 1G and H,), although these differences were not significant.

EZH2 knockdown sensitized EGFR-wt LUAD cells to gefitinib and suppressed cell viability and proliferation *in vitro*

To test whether *EZH2* affects the sensitivity of LUAD cells to EGFR-TKI, we knocked down *EZH2* expression in lung cancer cells using siRNA and subjected the cells to CCK8 assay after exposure to different concentrations of gefitinib for 24–48 h. As shown in Figure 2A and B, *EZH2* expressions in A549 and H1299 cells were significantly knocked down by *EZH2* siRNA. Using CCK8 assay, the viability of these cells was compared with that of cells treated with scrambled control siRNA and different gefitinib concentrations. As shown in Figure 2C and D, the si*EZH2* group was more sensitive to gefitinib than the siNC control group. The IC_{50} of gefitinib in A549 cells decreased from 44.7 μmol/L before knockdown to 31.0 μmol/L after knockdown (P = 0.026), and the IC_{50} of gefitinib in H1299 cells decreased from 32.02 μmol/L before knockdown to 23.97 μmol/L after knockdown (P< 0.01). These results indicated that *EZH2* knockdown sensitizes EGFR-wt LUAD cells to gefitinib.

Next, DZNep and GSK343 were applied to A549 and H1299 cells (Figure 2E). To further determine whether these drugs enhanced the antitumor effects of gefitinib in EGFR-wt lung cancer cells, we studied the effects of *EZH2* and EGFR co-inhibition on the viability of A549 and H1299 cells using CCK8 assay. We divided the cells into NC (10% serum medium alone), GSK343 (11 μmol/L GSK343), DZNep (10 μmol/LDZNep), gefitinib (12 μmol/L gefitinib), G+g (11 μmol/L GSK343+12 μmol/Lgefitinib), and D+g (10 μmol/L DZnep+12 μmol/Lgefitinib). CCK-8 assay revealed IC_{50} values of 20.14, 19.85, and 23.62 μmol/L for GSK343, DZNep, and gefitinib, respectively, in A549 cells, and corresponding values of 22.40, 24.97, and 36.15 μmol/L, respectively, in H1299 cells. CCK-8 assay showed that compared with NC, A549 cell viability rate was 87.39 ± 2.68, 78.04 ± 2.69, 70.65 ± 2.35, 44.11 ± 5.09, and 58.75 ± 2.05 for GSK343, DZNep, gefitinib, G+g, and D+g, respectively; in H1299 cells, the corresponding values were 77.66 ± 2.79, 84.14 ± 3.43, 65.75 ± 2.5, 42.99 ± 4.86, and 58.14 ± 1.81, respectively. The results indicated that the co-administration of GSK343 with gefitinib more effectively reduced cell viability than administration of gefitinib alone (P< 0.01 for both cell lines), whereas the co-administration of DZNep with gefitinib inhibited cell viability more significantly (A549, P< 0.01; H1299, P< 0.05; Figure 3A).

EdU assays were also performed to examine the effect of co-inhibition on cell proliferation activity (Figure 3B and C). In A549 cells, the mean number of EdU-positive cells in NC, GSK343, gefitinib, DZNep, G+g, and D+g was 51.92 ± 1.64, 44.9 ± 6.97, 47.83 ± 3.2, 30.15 ± 4.67, 6.93 ± 2.36, and 16.16 ± 1.09, respectively. The combined effects of GSK343+gefitinib or D+g on cell viability were greater than that of gefitinib alone (P< 0.01 for both). In H1299 cells, the mean number of EdU-positive cells in NC, GSK343, gefitinib, DZNep, G+g, and D+g was 52.07 ± 2.99, 41.93 ± 6.67, 40.63 ± 0.73, 44.47 ± 5.82, 11.95 ± 1.51, and 29.66 ± 3.13, respectively. Co-administration of GSK343+gefitinib or D+g was significantly more effective than administration of gefitinib alone (P< 0.01 for both).

Colony formation assays were performed to determine the effects of drug co-inhibition on cell proliferation. The treatment group was divided into six groups as described above. Cells were treated differently according to the previously mentioned drug concentration for 48 h. As shown in Figure 3D, 42.33 ± 2.52, 35.67 ± 1.53, 11.67 ± 1.53, 0 ± 0, and 3 ± 1 colonies formed in GSK343, DZNep, gefitinib, G+g, and D+g and these values were significantly lower than those in NC (76.33 ± 1.53; P < 0.01).

Co-administration of *EZH2* inhibitors with gefitinib enhanced apoptosis of EGFR-wt A549 and H1299 cells

Because the co-administration of an *EZH2* inhibitor with gefitinib sensitized the EGFR-wt lung cancer cells to gefitinib, we further investigated whether this treatment could also enhance the apoptosis of lung cancer cells. As illustrated in Figure 4Aand B, the apoptosis rates of A549 cells in NC, GSK343, DZnep, gefitinib, G+g, and D+g groups were 8.59 ± 2.25, 11.9 ± 3.15, 11.63 ± 1.7, 17.03 ± 3.34, 83.51 ± 3.71, and 57.24 ± 0.98, respectively. Here, the apoptosis rates in gefitinib, G+g, and D+g were significantly higher than those in NC (P = 0.02, <0.01, and <0.01, respectively). Moreover, G+g and D+g

were significantly more effective than gefitinib alone in this regard (P< 0.01 for both). Neither GSK343 nor DZNep alone had a significant effect on apoptosis rate (P = 0.21 and 0.14, respectively). Regarding H1299 cells, the apoptosis rates in NC, GSK343, DZnep, gefitinib, G+g, and D+g were 6.32 ± 2.32, 8.71 ± 2.17, 6.08 ± 0.83, 11.91 ± 1.93, 41.77 ± 3.1, and 16.87 ± 0.6, respectively. Gefitinib, G+g, and D+g had significantly stronger effects on apoptosis rate than NC (P = 0.03, <0.01, and <0.01, respectively). Co-administration of GSK343 with DZNep with gefitinib had more significant effects than the administration of gefitinib alone (P< 0.01 for both). However, single administration of neither *EZH2* inhibitor had an obvious effect on apoptosis rate (P = 0.26 and 0.88, respectively). Next, we detected the levels of the apoptosis-related proteins Bcl-2, Bax, and Caspase-3 in cells treated as described above. Unfortunately, we did not observe any significant changes in their levels in treated cells relative to NC-treated cells (Figure 4C).

Co-administration of *EZH2* inhibitors with gefitinib inhibits EGFR-wt lung cancer cell migration *in vitro*

We performed wound healing and transwell assays to explore the effects of co-administration of *EZH2* inhibitor with gefitinib treatment on the migratory abilities of EGFR-wt lung cancer cells. Wound healing assay revealed that the migratory abilities of H1299 cells in GSK343, DZNep, and gefitinib significantly decreased compared with those of cells in NC (54.77 ± 4.71, 54.33 ± 4.35, and 67.47 ± 2.54 vs. 82.47 ± 5.3, P = <0.01, <0.01, and 0.01, respectively; Figure 5A and B). Co-administrationof GSK343 or DZNep with gefitinib had significantly stronger inhibitory effects on cell migratory ability than the administrationof gefitinib alone (P< 0.01 for both). The rates of migrated cells in GSK343, DZNep, gefitinib, D+g, and G+g were 255 ± 12.99, 229 ± 18.19, 265.33 ± 21.03, 145.67 ± 19.5, and 126.67 ± 20.21, respectively. All combination groups had significantly greater decreases in cell migratory ability than NC (P< 0.01 for both; Figure 5C and D). Collectively, our data demonstrated that *EZH2* inhibitors (*EZH2* and DZNep), when administered in combination with EGFR inhibitors, can inhibit the migration of EGFR-wt NSCLC cells.

Co-administration of drugs suppressed *EZH2* and EGFR signaling pathways

To explore the possible mechanism underlying the abovementioned findings, we next evaluated changes in EGFR signaling pathway-related proteins. As shown in Figure 6A, A549 and H1299 cells were treated with different concentrations of gefitinib after *EZH2* knockdown (si*EZH2*) and subjected to western blotting. The results indicated that in both cell lines, co-administration of drugsslightly suppressed EGFR expression and strongly reduced *EZH2* protein expression and EGFR phosphorylation levels. The phosphorylation of AKT, a downstream molecule of EGFR, was also inhibited by the co-administration of drugs. These results proved that in A549 and H1299 cells treated with increasing concentrations of gefitinib, the levels of p-EGFR, *EZH2*, and p-AKT dramatically decreased, although the levels of AKT and EGFR were not significantly changed. The levels of P38-MAPK, an important signaling pathway downstream of EGFR, and p-P38-MAPK also did not change significantly. The levels of EGFR, p-EGFR, and p-AKT were lower in cells subjected to *EZH2* knockdown (si*EZH2*) and gefitinib treatment than in those in the control group (siNC; Figure 6).

Co-administration of GSK343 or DZNep with gefitinib suppressed the growth of EGFR-wt NSCLC *in vivo*

To further examine whether the co-administration of *EZH2* inhibitors with gefitinib would inhibit tumor growth *in vivo*, we established a BALB/c mouse lung neoplasm xenograft model using A549 cells. As shown in Figure 7A, GSK343, DZNep, and gefitinib monotherapies all had inhibitory effects on tumor growth (P < 0.01 for all). However, co-administration of GSK343 (4 mg/kg) or DZNep (2 mg/kg) with gefitinib (100 mg/kg) inhibited tumor growth significantly (P< 0.01, Figure 7A). After 28 days of treatment, the combination groups had a tumor volume of <280 mm^3, and 10% (1/10) of the mice in G+g had been completely cured. No severe adverse effects were observed in any of the combination groups. To further investigate the mechanism underlying tumor suppression, we analyzed xenograft tumor sections using immunohistochemistry to verify *EZH2* protein expression. Notably, we observed strongly reduced *EZH2* expression in G+g and D+g compared with in gefitinib (both P< 0.01; Figure 7B). In conclusion, the abovementioned results indicated that treatment the co-administration of *EZH2* inhibitors with gefitinib inhibited lung cancer cell growth *in vivo* by inhibiting *EZH2*.

Discussion

Lung cancer is among the most common and deadly cancers worldwide. NSCLC is the most common histological type of lung cancer, with LUSC and LUAD being the most common subtypes [25].Although the techniques used to diagnose lung cancer and surgical, radiotherapeutic, and chemotherapeutic treatment methods have significantly improved, the 5-year OS rates of patients with lung cancer remain as low as approximately 15% [3, 14, 26-28]. Tumor recurrence and metastasis present marked challenges to clinicians and severely affect the prognosis of patients. Approximately 70% of patients with lung cancer experience different degrees of focal metastasis and local tumor recurrence after tumor resection and adjuvant treatment. The most important cause of recurrence and metastasis involves the development of different degrees of drug resistance such that the original drug treatment can no longer inhibit and kill the tumor cells, leading to further disease progression. Therefore, researchers must explore new therapeutic methods and develop new anticancer drugs. Molecular targeted drugs have revolutionized lung cancer treatment. EGFR-TKIs are the most representative class of targeted therapies. Compared with traditional chemotherapy, EGFR-TKIs effectively treat advanced NSCLC with EGFR mutations and significantly prolong OS of patients [29-31]. However, the application of EGFR-TKIs also has some certain limitations. First, there are restrictions to achieving the treatment objective because patients must have specific EGFR gene mutations to benefit from EGFR-TKI therapy. Second, during the 9- to 14-month period after a good initial response to an EGFR-TKI, most patients eventually develop resistance to the drug [32]. Recent studies have demonstrated that EGFR-TKIs also have a certain inhibitory effect on EGFR-wt cancer cells. Therefore, EGFR-TKIs are considered second-line treatment options for patients with EGFR-wt cancers [33-36]. Nevertheless, current mainstream research is focused on the suitability of EGFR-TKIs for EGFR-wt cancers and whether these drugs can be combined with

other drugs to enhance their efficacy. In this study, we determined that gefitinib, a representative first-generation EGFR-TKI, can still exert antitumor effects in EGFR-wt NSCLC. These drugs not only inhibit cell viability but also inhibit cell migration and induce apoptosis in EGFR-wt A549 and H1299 cells; moreover, these effects can be enhanced by the co-administration of *EZH2* inhibitorswith gefitinib.

Developments in molecular biology and epigenetics have enabled researchers to determine that some special epigenetic trait changes (e.g., gene methylation and acetylation) will be present in tumors even if specific genetic locus changes (such as *KRAS* mutations) are excluded [37-39]. Epigenetic regulation plays an important role in cell growth, proliferation, differentiation, and apoptosis as well as an irreplaceable role in tumorigenesis and tumor development [40-42]. *EZH2* was identified as an important epigenetic regulatory gene that regulates histone methyltransferase activity and methylation modification. *EZH2* was originally identified in *Zeste*. Continuous exploration later revealed the presence of *EZH2* in the human body, and abnormal *EZH2* expression was detected frequently in a range of solid tumors including prostate cancer, breast cancer, kidney cancer, lung cancer, and lymphoma [43, 44]. *EZH2* is a polycomb protein homologous to the *Drosophila* enhancer of *zeste* and catalyzes the addition of methyl groups to H3K27. *EZH2* plays important roles in tumorigenesis and cancer progression through epigenetic gene silencing and chromatin remodeling. *EZH2* overexpression has been reported in various human malignancies including NSCLC and may be associated with worse outcomes [6, 11, 45-47]. Numerous studies have analyzed the correlation between *EZH2* expression and lung cancer prognosis. The general consensus is that *EZH2* expression level is negatively correlated with the prognosis of patients with NSCLC [15, 48-50]. In this study, we determined the differences in *EZH2* expression levels between paired tumor and paracancerous lung tissues using the TCGA database. When compared with paracancerous lung tissues, LUAD and LUSC expressed higher *EZH2* expression levels. The results of TCGA database analysis also indicated that a higher *EZH2* expression level was related to poor prognosis only in LUAD, which is inconsistent with the findings of previous studies [50, 52]. In addition, our clinical data analysis revealed a trend toward shorter OS in patients with higher *EZH2* expression levels.

Given the important role of *EZH2* in tumorigenesis and development, researchers have developed various *EZH2* inhibitors and evaluated these through *in vitro* experiments and clinical studies. *EZH2* inhibitors can enhance the sensitivity of tumor cells to antitumor drugs and thereby enhance the efficacy of the drugs. *EZH2* has been reported to play an important role in the acquired resistance of tumor cells to chemotherapeutic drugs in small-cell lung cancer. For example, Gardner et *al*. reported that chemotherapeutic drugs induced the accumulation of H3K27me3 on *SLFN11* through the methylation of *EZH2*, which led to partial chromatin condensation and inhibited *EZH2* expression [53]. In NSCLC, *EZH2* inhibitors could effectively enhance sensitivity to etoposide in patients with BRG1- and EGFR-mutant lung cancers [49]. The inhibition of *EZH2* expression could effectively reverse resistance to platinum-based chemotherapy in NSCLC [54].The combination of the *EZH2* inhibitor DZNep and histone deacetylase inhibitor Novelitar could significantly suppress NSCLC cell proliferation and induced apoptosis [17]. *EZH2* inhibitors also enhanced sensitivity to soracinib in hepatoma carcinoma cells [55]. In this study, we found that *EZH2* silencing enhanced gefitinib sensitivity in gefitinib-resistant cells. To further investigate the effects of a combination of an *EZH2* inhibitor and gefitinib on primary gefitinib-resistant cells, we treated the EGFR-wt NSCLC cell lines A549 and H1299 with the *EZH2* inhibitors DZNep and GSK343. The co-administration of either inhibitor with gefitinib more strongly inhibited cell proliferation and migration than any single drug. In addition, co-treatment significantly inhibited the phosphorylation of AKT, which is activated downstream of EGFR. We also found that the co-administration of *EZH2* inhibitors with gefitinib exerted good tumor-suppressing effects against primary gefitinib-resistant cells *invivo*.

Lung cancer remains a life-threatening malignancy in humans. EGFR-targeted drugs have provided new treatment options for these tumors. *EZH2* inhibitors have also provided new treatment concepts. In this study, we found that a therapeutic combination of an *EZH2* inhibitor and gefitinib could significantly inhibit tumor growth and metastasis in primary gefitinib-resistant cells both *in vivo* and *in vitro*. Our findings indicate a new direction for the future clinical treatment of lung cancer.

Conclusions

Taken together, Our study reveal thatco-administration of EZH2 inhibitors with EGFR-TKIs may be feasible for the treatment of EGFR wild-type NSCLC in patients who refuse traditional chemotherapy.

Abbreviations

NSCLC:Non-small-cell lung cancer;LUAD:lung adenocarcinoma.LUSC,lung squamous cell carcinoma;EGFR-TKI:epidermal growth factor receptor (EGFR)-tyrosine kinase inhibitors;KRAS:Kirsten Rat Sarcoma Viral Proto-Oncogene; EZH2:Enhancer of zeste homolog 2;PRC2:polycomb suppression complex 2;TCGA:The Cancer Genome Atlas;wt:wild-type;OS:over survival.

Declarations

Ethics approval and consent to participate

This study was approved by the Ethical Review Committee of Tianjin Medical University General Hospital. All biological samples were obtained with patients' written informed consent. All animal procedures and experimental protocols were approved by Laboratory Animal Ethics Committee of Tianjin Medical University.

Consent for publication

Not applicable.

Availability of data and material

All data generated or analysed during this study are included in this published article.

Competing interests

The authors declare that they have no competing interests.

Funding

This study was supported by grants from the National Natural Science Foundation of China (81773207 and 61973232), Natural Science Foundation of Tianjin (17YFZCSY00840, 18PTZWHZ00240, 19YFZCSY00040, and 19JCYBJC27000), and Special Support Program for the High Tech Leader and Team of Tianjin (TJTZJH-GCCCXCYTD-2-6). The funding sources had no role in study design, data collection, and analysis; the decision to publish; or the preparation of the manuscript.

Authors' contributions

JC and HYL designed and supervised of the study. HG, YWL, HYL and JC wrote the manuscript. YY, WTL, YWL and HBZ performed the experiments. RFS, ZHZ MHL and CL helped to perform some experiments. All authors analyzed the data together, discussed the manuscript and approved the final manuscript.

Acknowledgements

Not applicable.

References

1. Bray F,Ferlay J,Soerjomataram I,Siegel RL, Torre LA, Jemal A.Global cancer statistics 2018: GLOBOCAN estimates of incidence and mortality worldwide for 36 cancers in 185 countries.CA Cancer J Clin. 2018; 68(6): 394-424.
2. Torre LA,Bray F,Siegel RL,Ferlay J,Lortet-Tieulent J, Jemal A.Global cancer statistics,2012.CA Cancer J Clin.2015; 65(2): 87-108.
3. Siegel RL,Miller KD,Jemal A.Cancer statistics, 2018.CA Cancer J Clin. 2018; 68(1): 7-30.
4. Verdecchia A,Francisci S,Brenner H,Gatta G,Micheli A,Mangone L,et al. Recent cancer survival in Europe: a 2000-02 period analysis of EUROCARE-4 data.Lancet Oncol.2007; 8(9): 784-96.
5. Waldmann T,Schneider R.Targeting histone modifications--epigenetics in cancer.Curr Opin Cell Biol.2013; 25(2): 184-9.
6. McCabe MT,Mohammad HP,Barbash O,Kruger RG.Targeting Histone Methylation in Cancer.Cancer J. 2017; 23(5): 292-301.
7. Feinberg AP,Vogelstein B.Hypomethylation distinguishes genes of some human cancers from their normal counterparts.Nature.1983; 301(5895): 89-92.
8. Chen Y,Liu X,Li Y,Quan C,Zheng L,Huang K.Lung Cancer Therapy Targeting Histone Methylation: Opportunities and Challenges.Comput Struct Biotechnol J.2018;16: 211-23.
9. Margueron R,Reinberg D.The Polycomb complex PRC2 and its mark in life. Nature.2011;469(7330): 343-9.
10. Huqun, Ishikawa R, Zhang J, Miyazawa H,Goto Y,Shimizu Y,et al. Enhancer of zeste homolog 2 is a novel prognostic biomarker in nonsmall cell lung cancer. Cancer. 2012; 118(6): 1599-606.
11. Behrens C, Solis LM, Lin H,Yuan P, Tang X, Kadara H, et al. EZH2 protein expression associates with the early pathogenesis, tumor progression, and prognosis of non-small cell lung carcinoma. Clin Cancer Res. 2013; 19(23): 6556-65.
12. Zhang Y, Lin C, Liao G,Liu S, Ding J, Tang F, et al. MicroRNA-506 suppresses tumor proliferation and metastasis in colon cancer by directly targeting the oncogene EZH2. Oncotarget. 2015; 6(32): 32586-601.
13. Chase A, Cross NC. Aberrations of EZH2 in cancer. Clin Cancer Res. 2011; 17(9): 2613-8.
14. Xu C, Hou Z, Zhan P, Zhao W, Chang C, Zou J, et al. EZH2 regulates cancer cell migration through repressing TIMP-3 in non-small cell lung cancer. Med Oncol. 2013; 30(4): 713.
15. Takashina T, Kinoshita I, Kikuchi J, Shimizu Y, Sakakibara-Konishi J, Oizumi S, et al. Combined inhibition of EZH2 and histone deacetylases as a potential epigenetic therapy for non-small-cell lung cancer cells. Cancer Sci. 2016; 107(7): 955-62.
16. Kikuchi J, Kinoshita I, Shimizu Y, Kikuchi E, Konishi J, Oizumi S,et al. Distinctive expression of the polycomb group proteins Bmi1 polycomb ring finger oncogene and enhancer of zeste homolog 2 in nonsmall cell lung cancers and their clinical and clinicopathologic significance. Cancer. 2010; 116(12): 3015-24.
17. Miranda TB, Cortez CC, Yoo CB, Liang G, Abe M, Kelly T,et al. DZNep is a global histone methylation inhibitor that reactivates developmental genes not silenced by DNA methylation. Mol Cancer Ther. 2009; 8(6): 1579-88.

18. Wang Z, Candelora C. In Vitro Enzyme Kinetics Analysis of EGFR. Methods Mol Biol. 2017; 1487: 23-33.
19. Nan X, Xie C, Yu X, Liu J. EGFR TKI as first-line treatment for patients with advanced EGFR mutation-positive non-small-cell lung cancer. Oncotarget. 2017; 8(43): 75712-26.
20. Morgillo F, Della Corte CM, Fasano M, Ciardiello F. Mechanisms of resistance to EGFR-targeted drugs: lung cancer. ESMO Open. 2016; 1(3): e000060.
21. Zhou Q, Cheng Y, Yang JJ, Zhao MF , Zhang L , Zhang XC, et al. Pemetrexed versus gefitinib as a second-line treatment in advanced nonsquamous nonsmall-cell lung cancer patients harboring wild-type EGFR (CTONG0806): a multicenter randomized trial. Ann Oncol. 2014; 25(12): 2385-91.
22. Sequist LV, Yang JC, Yamamoto N, O'Byrne K, Hirsh V, Mok T,et al. Phase III study of afatinib or cisplatin plus pemetrexed in patients with metastatic lung adenocarcinoma with EGFR mutations. J Clin Oncol. 2013; 31(27): 3327-34.
23. Sun J, Nishiyama T, Shimizu K, Kadota K. TCC: an R package for comparing tag count data with robust normalization strategies. BMC Bioinformatics. 2013; 14: 219.
24. Naito S, von Eschenbach AC, Giavazzi R, Fidler IJ. Growth and metastasis of tumor cells isolated from a human renal cell carcinoma implanted into different organs of nude mice. Cancer Res. 1986; 46(8): 4109-15.
25. Herbst RS, Heymach JV, Lippman SM. Lung cancer. N Engl J Med. 2008; 359(13): 1367-80.
26. Duma N, Davila RS, Molina JR. Non-Small Cell Lung Cancer: Epidemiology, Screening, Diagnosis, and Treatment.Mayo Clin Proc. 2019; 94(8):1623-40.
27. Liao Y, Fan X, Wang X. Effects of different metastasis patterns, surgery and other factors on the prognosis of patients with stage IV non-small cell lung cancer: A Surveillance, Epidemiology, and End Results (SEER) linked database analysis. Oncol Lett. 2019; 18(1): 581-592.
28. Duma N, Santana-Davila R, Molina JR. Non-Small Cell Lung Cancer: Epidemiology, Screening, Diagnosis, and Treatment. Mayo Clin Proc. 2019; 94(8): 1623-1640.
29. Wang C, Wang T, Lv D, Li L, Yue JN, Chen HZ, et al. Acquired resistance to EGFR TKIs mediated by TGF-beta1/integrin beta3 signaling in EGFR-mutant lung cancer. Mol Cancer Ther. 2019; 18(12):2357-67.
30. Saida Y, Watanabe S, Abe T, Shoji S, Nozaki K, Ichikawa K, et al. Efficacy of EGFR-TKIs with or without upfront brain radiotherapy for EGFR-mutant NSCLC patients with central nervous system metastases. Thorac Cancer. 2019;10(11):2106-16.
31. Cheng H, Li XJ, Wang XJ,Chen ZW, Wang RQ, Cheng H, et al. A meta-analysis of adjuvant EGFR-TKIs for patients with resected non-small cell lung cancer. Lung Cancer. 2019; 137: 7-13.
32. Liu M, Xu S, Wang Y, Li Y, Li YW, Zhang HZ, et al. PD 0332991, a selective cyclin D kinase 4/6 inhibitor, sensitizes lung cancer cells to treatment with epidermal growth factor receptor tyrosine kinase inhibitors. Oncotarget. 2016; 7(51): 84951-84964.
33. Cross DA, Ashton SE, Ghiorghiu S, Eberlein C, Nebhan CA, Spitzler PJ, et al. AZD9291, an irreversible EGFR TKI, overcomes T790M-mediated resistance to EGFR inhibitors in lung cancer. Cancer Discov. 2014; 4(9): 1046-61.
34. Walter AO, Sjin RT, Haringsma HJ, Ohashi K, Sun J, Lee K,et al. Discovery of a mutant-selective covalent inhibitor of EGFR that overcomes T790M-mediated resistance in NSCLC. Cancer Discov. 2013; 3(12): 1404-15.
35. Tjin Tham Sjin R, Lee K, Walter AO, Dubrovskiy A, Sheets M, Martin TS ,et al. In vitro and in vivo characterization of irreversible mutant-selective EGFR inhibitors that are wild-type sparing. Mol Cancer Ther. 2014; 13(6): 1468-79.
36. Paz-Ares LG, de Marinis F, Dediu M, Thomas M, Pujol JL, Bidoli P, et al. PARAMOUNT: Final overall survival results of the phase III study of maintenance pemetrexed versus placebo immediately after induction treatment with pemetrexed plus cisplatin for advanced nonsquamous non-small-cell lung cancer. J Clin Oncol. 2013; 31(23): 2895-902.
37. Decourcelle A, Leprince D, Dehennaut V. Regulation of Polycomb Repression by O-GlcNAcylation: Linking Nutrition to Epigenetic Reprogramming in Embryonic Development and Cancer. Front Endocrinol (Lausanne). 2019; 10: 117.
38. Jiao J, Sagnelli M, Shi B, Fang YY, Shen ZQ, Tang TY, et al. Genetic and epigenetic characteristics in ovarian tissues from polycystic ovary syndrome patients with irregular menstruation resemble those of ovarian cancer. BMC Endocr Disord. 2019; 19(1): 30.
39. Fritz AJ, Gillis NE, Gerrard DL, Rodriguez PD, Hong D, Rose JT, et al. Higher order genomic organization and epigenetic control maintain cellular identity and prevent breast cancer. Genes Chromosomes Cancer. 2019 ;58(7):484-99.
40. Zhang L. Linking metabolic and epigenetic regulation in the development of lung cancer driven by TGFβ signaling. AIMS Genet. 2019; 6(2): 11-13.
41. Cai L, Bai H, Duan J, Wang ZJ, Gao SG, Wang D, et al. Epigenetic alterations are associated with tumor mutation burden in non-small cell lung cancer. J Immunother Cancer. 2019; 7(1): 198.
42. Naqvi S, Kim Y. Epigenetic modification by galactic cosmic radiation as a risk factor for lung cancer: real world data issues. Transl Lung Cancer Res. 2019; 8(2): 116-118.
43. Yu Y, Qi J, Xiong J, Jiang LP, Cui D, He JL, et al. Epigenetic Co-Deregulation of EZH2/TET1 is a Senescence-Countering, Actionable Vulnerability in Triple-Negative Breast Cancer. Theranostics; 2019; 9(3): 761-777.
44. Batool A, Jin C, Liu YX. Role of EZH2 in cell lineage determination and relative signaling pathways. Front Biosci (Landmark Ed). 2019; 24: 947-960.
45. Park KS, Kim HK, Lee JH, Choi YB, Park SY, Yang SH, et al. Transglutaminase 2 as a cisplatin resistance marker in non-small cell lung cancer. J Cancer Res Clin Oncol. 2010; 136(4): 493-502.
46. Hussein YR, Sood AK, Bandyopadhyay S, Albashiti B, Semaan A, Nahleh Z, et al. Clinical and biological relevance of enhancer of zeste homolog 2 in triple-negative breast cancer. Hum Pathol. 2012; 43(10): 1638-44.

47. Xu C, Hao K, Hu H, Sheng ZH, Yan J, Wang QB,et al. Expression of the enhancer of zeste homolog 2 in biopsy specimen predicts chemoresistance and survival in advanced non-small cell lung cancer receiving first-line platinum-based chemotherapy. Lung Cancer. 2014; 86(2): 268-73.
48. Ihira K, Dong P, Xiong Y, Watari H, Konno Y, Hanley SJ, et al. EZH2 inhibition suppresses endometrial cancer progression via miR-361/Twist axis. Oncotarget. 2017; 8(8): 13509-13520.
49. Fillmore CM, Xu C, Desai PT, Berry JM, Rowbotham SP, Lin YJ, et al. EZH2 inhibition sensitizes BRG1 and EGFR mutant lung tumours to TopoII inhibitors. Nature. 2015; 520(7546): 239-42.
50. Wang X, Zhao H, Lv L, Bao L, Wang X, Han S. Prognostic Significance of EZH2 Expression in Non-Small Cell Lung Cancer: A Meta-analysis. Sci Rep. 2016; 6: 19239.
51. Li Z, Xu L, Tang N, Xu YH, Ye XY, Shen SP, et al. The polycomb group protein EZH2 inhibits lung cancer cell growth by repressing the transcription factor Nrf2. FEBS Lett. 2014; 588(17): 3000-7.
52. Kim NY, Pyo JS. Clinicopathological significance and prognostic role of EZH2 expression in non-small cell lung cancer. Pathol Res Pract. 2017; 213(7): 778-782.
53. Gardner EE, Lok BH, Schneeberger VE, Desmeules P, Miles LA, Arnold PK, et al. Chemosensitive Relapse in Small Cell Lung Cancer Proceeds through an EZH2-SLFN11 Axis. Cancer Cell. 2017; 31(2): 286-299.
54. Liu H, Li W, Yu X,Gao F, Duan Z, Ma XL, et al. EZH2-mediated Puma gene repression regulates non-small cell lung cancer cell proliferation and cisplatin-induced apoptosis. Oncotarget. 2016; 7(35): 56338-56354.
55. Follis AV, Chipuk JE, Fisher JC,Yun MK, Grace CR, Nourse A, et al. PUMA binding induces partial unfolding within BCL-xL to disrupt p53 binding and promote apoptosis. Nat Chem Biol. 2013; 9(3): 163-8.

Figures

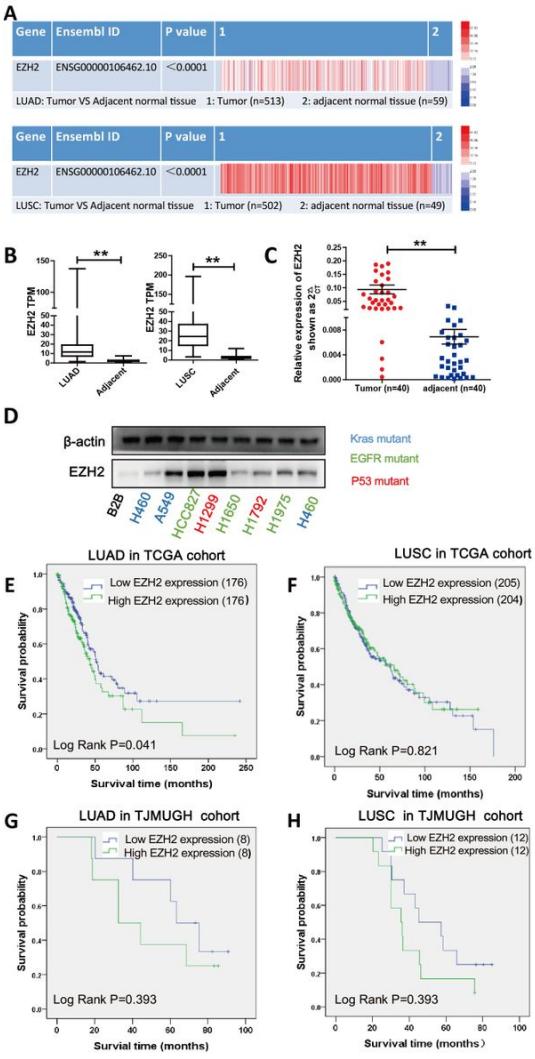

Figure 1

Enhancer of zeste homolog 2 (EZH2) is strongly expressed in non–small-cell lung cancer (NSCLC) and is associated with poor prognosis in patients with lung adenocarcinoma. A. Relative expression of EZH2 in NSCLC tissues compared with in paracancerous lung tissues in The Cancer Genome Atlas dataset. B. EZH2 TPM in NSCLC and paracancerous lung tissues in TCGA. C. EZH2 expression levels in NSCLC tissues (n = 40) compared with those in paracancerous lung tissues (n = 40) by qPCR analysis; data were normalized against GAPDH expression level. D. EZH2 protein levels in different NSCLC lines and the normal alveolar epithelial cell line BEAS-2B. E–F. Overall survival curves of patients with LUAD and LUSC from the TCGA cohort. G–H. Overall survival curves of patients with LUAD and LUSC from the TJMUGH cohort.

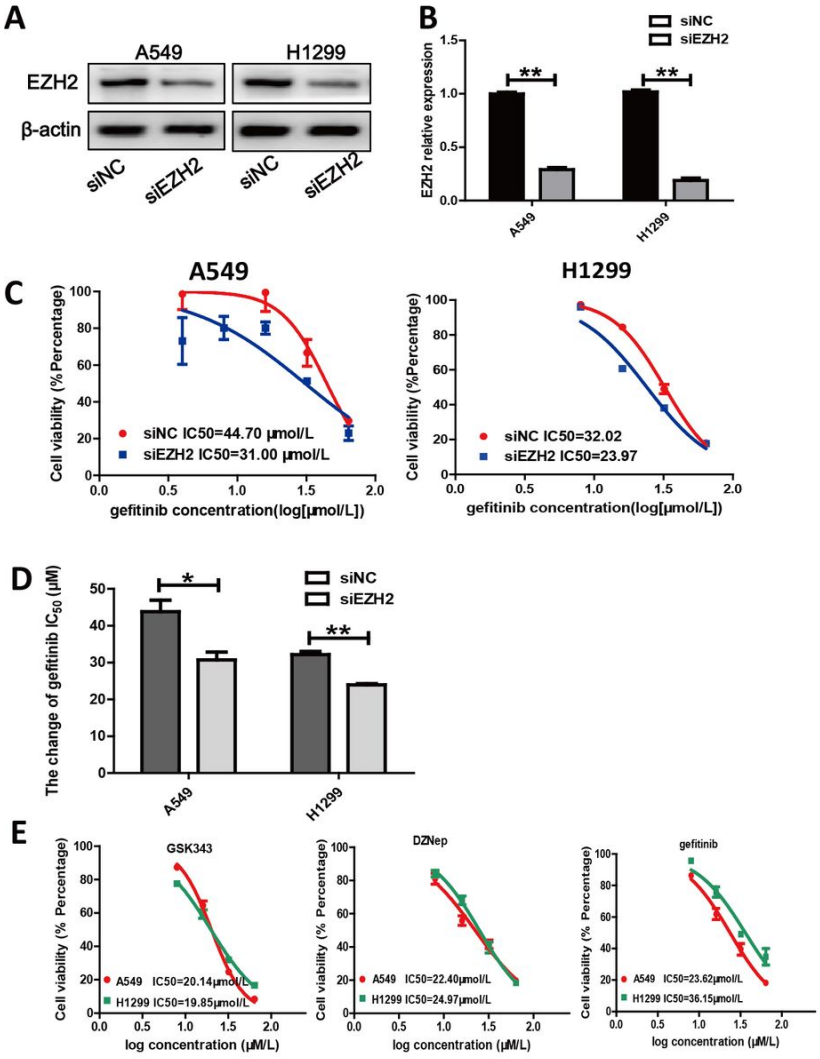

Figure 2

Enhancer of zeste homolog 2 (EZH2) knockdown increased sensitivity of EGFR wild-type A549 and H1299 cells to gefitinib. A. EZH2 protein levels were assessed by western blotting. B. Quantitative PCR analysis of relative EZH2 mRNA expression level normalized to GAPDH expression level. C. Proliferation of transfected EZH2 cells was measured using CCK-8 assay. D. Changes in drug IC50 values after EZH2 silencing. All results are presented as mean ± standard deviation (SD) of triplicate experiments. * P< 0.05, ** P< 0.01 vs. control group. E. CCK-8 analysis of cell lines treated with GSK343, DZNep, and gefitinib. Data are representative of three independent experiments. Data are presented as mean ± SD of triplicate samples.

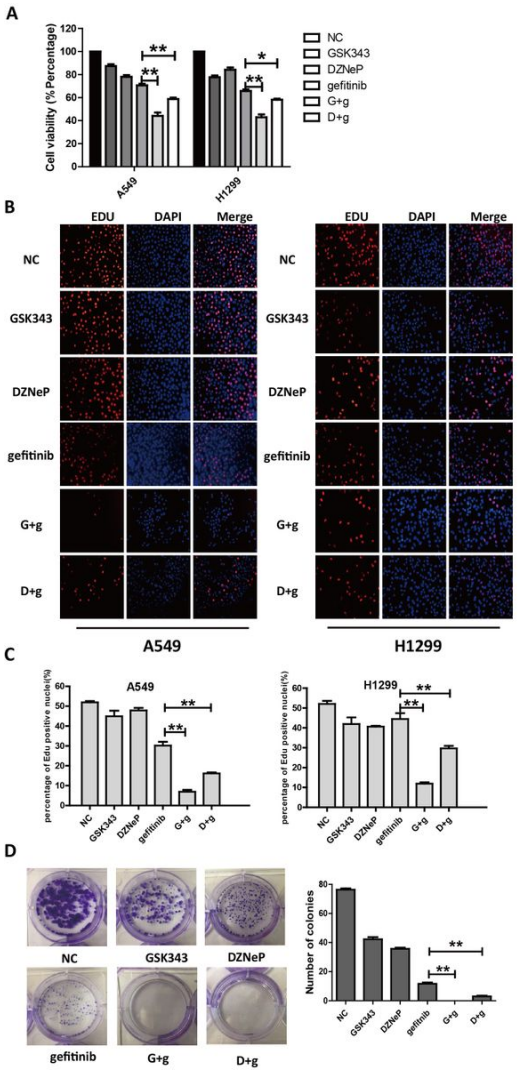

Figure 3

Co-administration of enhancer of zeste homolog 2 (EZH2) inhibitors with gefitinib significantly suppressed lung cancer cell growth in vitro. Cells were subjected to control treatment (NC), GSK343 (11 μmol/L), DZNep (10 μmol/L), gefitinib (12 μmol/L), G+g (11 μmol/L GSK343 + 12 μmol/L gefitinib), or D+g (10 μmol/L DZNep + 12 μmol/L gefitinib) for 48 h. A. Results of CCK-8 assay for cell lines treated as indicated. B–C. Results of EdU assay of cell lines treated with the indicated drug combinations. D. Colony formation assay was performed to test the effects of different treatments on the proliferation of A549 cells. Data are presented as mean ± standard deviation. * P< 0.05, ** P< 0.01 vs. scrambled control group.

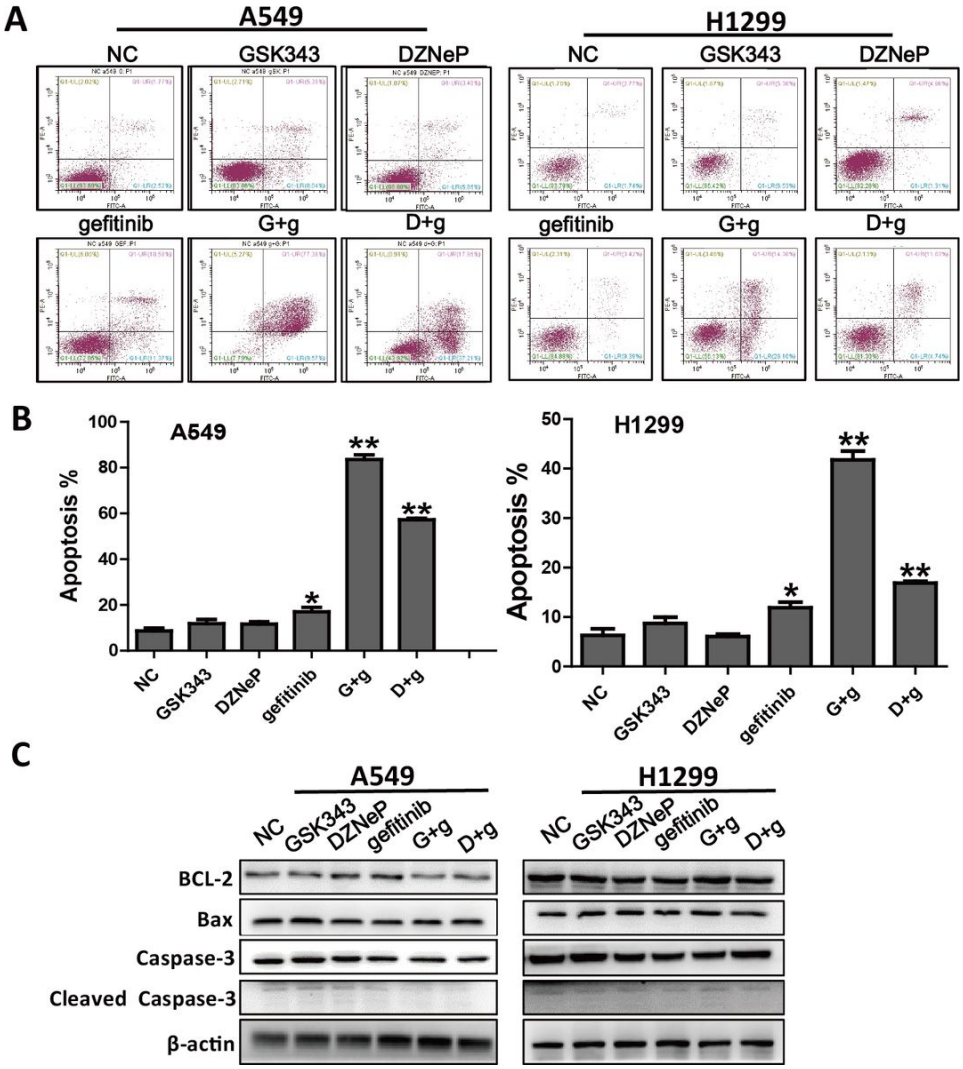

Figure 4

Enhancer of zeste homolog 2 (EZH2) inhibitors enhance gefitinib-induced apoptosis of primary gefitinib-resistant cell lines (A549 and H1299). A–B. Apoptosis was analyzed by flow cytometry analysis after 48 h of exposure to GSK343, DZNep, gefitinib, GSK343+gefitinib, and D+g. C. The effects of GSK343, DZNep, and gefitinib on Bcl-2, Bax, Caspase-3, and cleaved Caspase-3 protein levels in A549 and H1299 cells were evaluated by western blotting. Data are presented as mean ± standard deviation (n = 3 independent experiments). * P< 0.05, ** P< 0.01, *** P< 0.001 vs. control group.

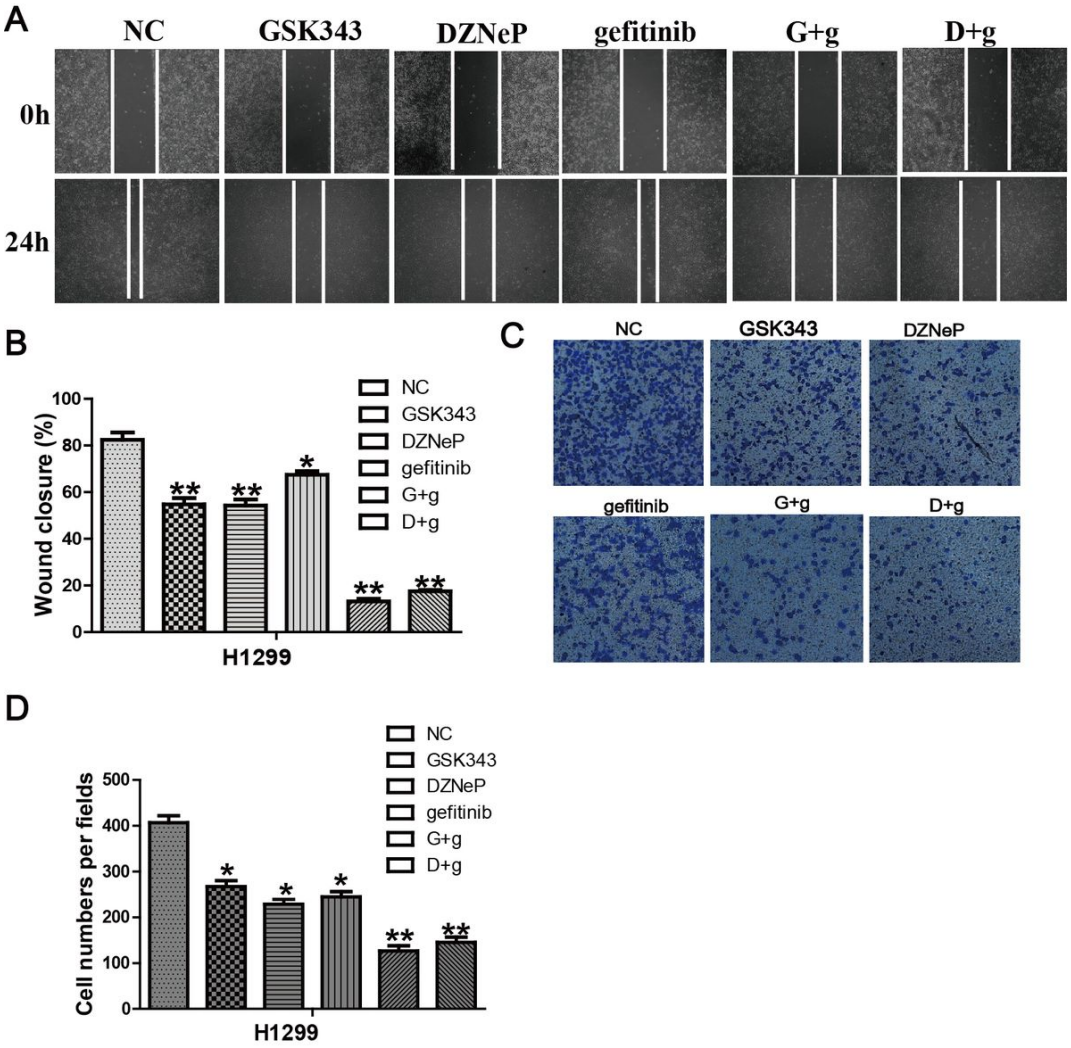

Figure 5

Combined treatment with enhancer of zeste homolog 2 (EZH2) inhibitors and epidermal growth factor receptor (EGFR) inhibitors inhibits EGFR wild-type lung cancer cell migration in vitro. A–B. Wound healing assay of A549 and H1299 cells treated with GSK343, DZNep, gefitinib, GSK343+gefitinib, or DZNep+gefitinib for 24 h. Representative images are displayed at 4× magnification. Scale bar = 800 μm. Data are presented mean ± standard deviation (SD). * P< 0.05, ** P< 0.01. C–D. Transwell migration assay of A549 cells treated as indicated for A and B. Data are presented as mean ± SD. Scale bar = 200 μm, and images were are displayed at 20× magnification, * P< 0.05, ** P< 0.01

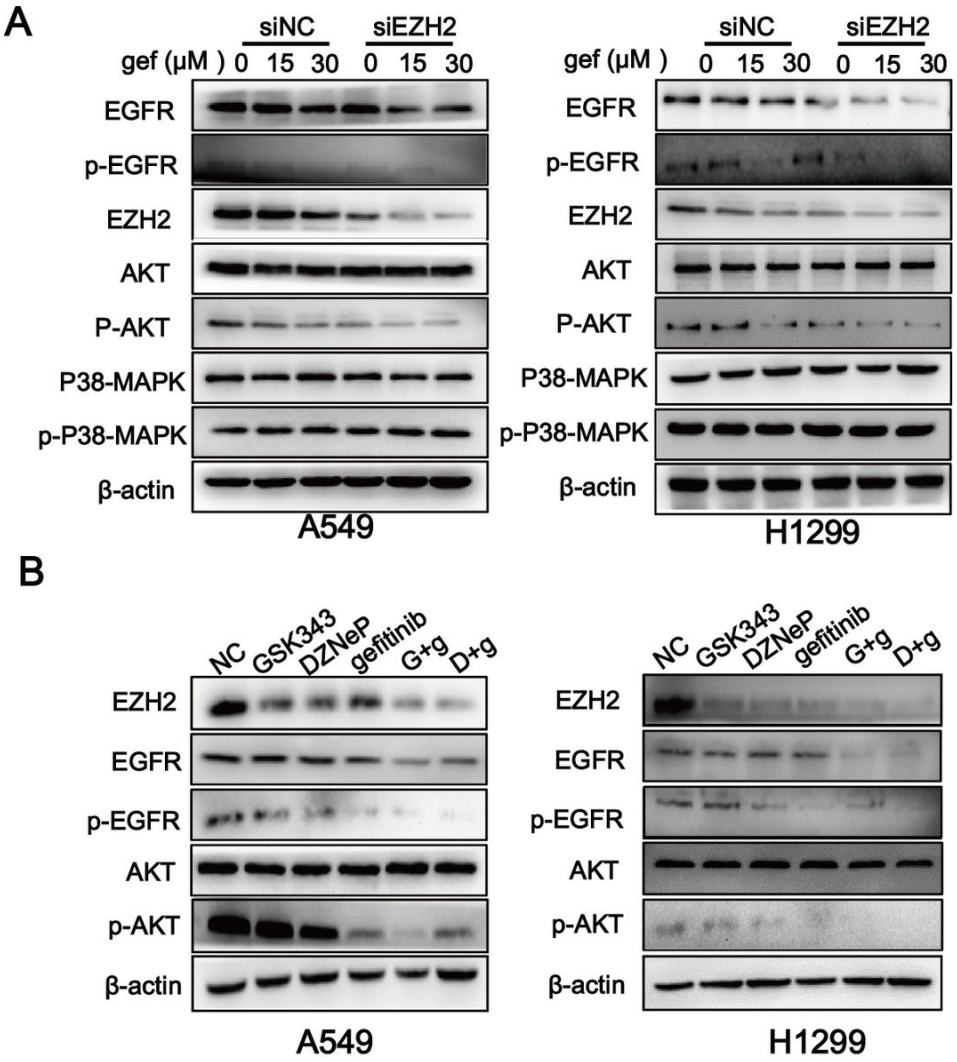

Figure 6

Co-administration of enhancer of zeste homolog 2 (EZH2) inhibitor with gefitinib suppressed EZH2 and EGFR signaling pathways. Cells were treated with GSK343 (11 μmol/L), DZNep (10 μmol/L), gefitinib (12 μmol/L), G+g (11 μmol/L GSK343 + 12 μmol/L gefitinib), or D+g (10 μmol/L DZNep + 12 μmol/L gefitinib). A and B. The effects of EZH2 knockdown on the levels of the EZH2 and the EGFR/AKT pathway components EGFR, AKT, and MAPK in A549 and H1299 cells were evaluated by western blotting. C and D. The effects of GSK343, DZNep, and gefitinib on the levels of proteins evaluated in A and B were evaluated in A549 and H1299 cells by western blotting.

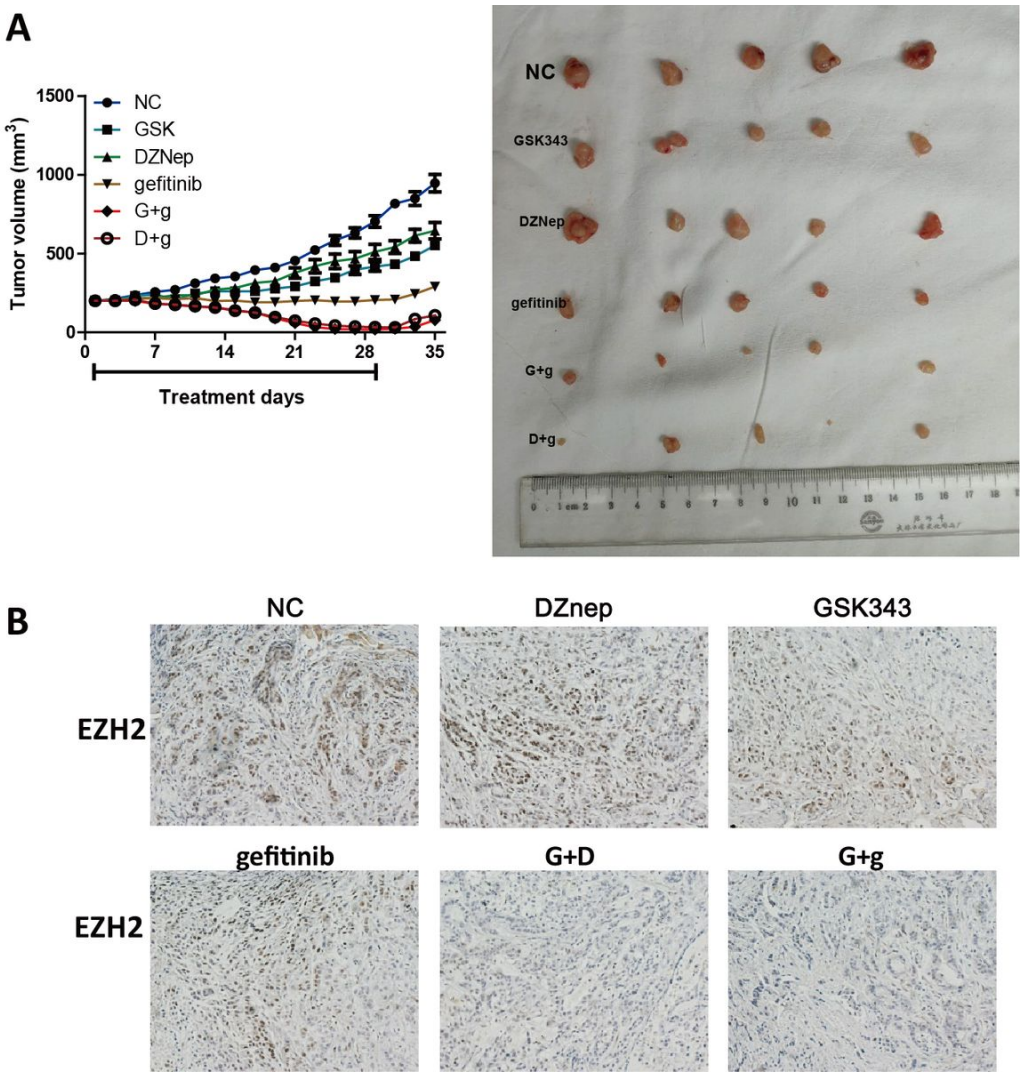

Figure 7

Effects of co-administration of enhancer of zeste homolog 2 (EZH2) inhibitors with gefitinib in vivo. A. Tumor volumes in mice were measured every 5 days. Results are presented as mean ± standard deviation. A total of 2 × 106 A549 cells were subcutaneously injected into the left flank of each mouse. When the tumors reached a volume of 200 mm3, mice were randomly assigned to six groups as indicated (10 mice/group) and treated with the corresponding drugs described in the Materials and Methods section. * P< 0.05, ** P< 0.01. B. Tumor sections were evaluated using immunohistochemistry with an EHZ2-specific antibody. The results shown represent three independent experiments.